

LAMB WAVE PROPAGATION IN RODS WITH DISCONTINUITIES

Magdalena Palacz

Institute of Fluid Flow Machinery PAS, Fiszerza 14, 80-952 Gdańsk, Poland
e-mail: mpal@imp.gda.pl

Joanna Grabowska

Institute of Fluid Flow Machinery PAS, Fiszerza 14, 80-952 Gdańsk, Poland
e-mail: jg@imp.gda.pl

Marek Krawczuk

Institute of Fluid Flow Machinery PAS, Fiszerza 14, 80-952 Gdańsk, Poland
Technical University of Gdansk, Department of Electrical Engineering and Automatic, Narutowicza 11/12, 80-952 Gdańsk, Poland
e-mail: mk@imp.gda.pl

Abstract. *Structural health monitoring and damage detection is very important from the maintenance of the constructional elements point of view. The main objective of the theoretical portion of this problem is to develop a model that will determine the relationship between the damage and the signal obtained in testing process. In case of wave propagation analysis so far used models based on the Finite Element Method are inefficient due to the computational effort. For that reason new models, based on the Spectral Element Method (SEM), are under consideration of many research centers. In the article the analysis of Lamb wave propagation in rods with discontinuities is presented. For that purpose new spectral element is developed. The above element is based on three different theories. A procedure of creating the dynamic stiffness matrix for the models is described in details. Numerical examples illustrate the wave propagation process in rods with fatigue crack, with the change of the cross section area and the change in material properties. The signal processing of the responses allows pointing out what kind of the discontinuity one has in the element tested.*

Keywords: *Lamb wave, Spectral Element Method.*

1. Introduction

Structural health monitoring and damage detection has received a considerable amount of interest over the last few decades. Previous approaches to non-destructive evaluation of structures, and assessing their integrity, typically involved some form of human interaction. Recent advances in smart materials technology resulted in a renewed interest in developing advanced self-diagnostic methods for assessing the state of a structure without any human interaction (Chang). The goal is to reduce the human contribution while monitoring the integrity of a structure. With this goal in mind, many researchers have made significant progress in developing damage detection methods for structures based on traditional modal analysis techniques. These techniques are often well suited for detection of rather big defects, because small defects do not influence changes in low frequencies, thus global behavior of the system is not affected. For this reason new methods based on smart materials have been rapidly developed in last years.

Wave propagation in structural elements has been studied over considerable period of time. Although mathematical frameworks are well developed wave propagation problems in real scale engineering structures is an open area of research. The main problems, in analyzing of propagation of high velocity waves in distributed structures, are that spatial discretisation must be accurate to capture the amplified effect of wave scattering at structural discontinuities. A conventional modal method, when extended to the high frequency regime, becomes computationally inefficient since many higher modes that participate in the motion will not be represented. For a specific geometry and finite, periodic or semi-infinite boundary conditions, many solution techniques have been reported (Bathe, M. Redwood, Cheung). Among many frequency domain methods, the Spectral Element Method (Doyle) has been found suitable for analysis of wave's propagation in real engineering structures.

The Spectral Element Method utilizes the exact solution of differential equations governing a problem. This exact solution is used as an interpolating function for the spectral element formulation. The use of the exact solution in the element formulation ensures the exact mass and stiffness distribution. It means that only one element can be used for modeling a very large part of the structure. Hence, the problem size is much smaller in comparison to the conventional Finite Elements formulation. For example, in order to model properly wave propagation with frequency about 200 kHz, in cantilever rod with length 6m and cross-section 0,02x0,02 m almost 465 rod finite elements is needed. It means that length of the one element is about 0,012 m, and it seems that they are not rods in a physical meaning. Obviously it is possible to use other types of finite elements (e.g. 3D-solids), but in this case the size of problem would be greater. What is also obvious the time of numerical calculations would be long, and errors of numerical integration could be considerable. The spectral analysis allows using one spectral element for any length, unless there is change in cross

section or material parameters. If something like that happens it is very simple to join several spectral elements in a way that is commonly used in finite elements method.

The spectral element program architecture is very similar to the technique of the finite element as far as the assembly and solution of equations is considered. Firstly, the excitation function is split up into a number of frequency components using the forward Fourier Transformation. Next, as a part of a big frequency do-loop (as opposed to a do-loop over time step in the conventional Finite Elements formulation), the dynamic stiffness matrix is generated, transformed and solved for unit impulses at each frequency. This yields directly to the Frequency Response Function of the analyzed problem. The frequency domain responses are then transformed to the time domain using the Inverse Fourier Transformation. The spectral elements are available for rods, and layered solids. For rod elements one can find spectral elements developed on the bases of elementary rod theory, however there are no spectral elements, which are based on modified theories. Such elements would be suitable for analysis of waves with higher frequencies. Apart from that they take into account more realistic assumption undergoing the longitudinal and transverse deformations. Problems of longitudinal waves propagation have been analysed up till now using the elementary theory that assumes a constant longitudinal displacement along the cross-section of the rod and also neglects a transverse deflection. The real deformation of the rod is more complicated, and in broad terms we can identify three distinct behaviors. The first is that the longitudinal displacement has a nonzero mean value (Love rod theory), the second is that the transverse deflection is nearly linear (Mindlin-Herrmann rod theory), and the third that the longitudinal displacement has almost a parabolic distribution (three-mode rod theory). It means that higher order theories should have two additional deformations modes – the transverse deflection and the parabolic longitudinal displacement along height of the rod.

In the present paper new spectral elements for analysis of longitudinal waves in rods and in rods with fatigue cracks are developed. The elements are based on the Love and Mindlin-Herrmann rod theories (Doyle). In case of the Love rod theory, the spectral element has two nodes and one longitudinal degree of freedom at a node. For the Mindlin-Herrmann rod theory the spectral element has two nodes and two degrees of freedom at a node – the longitudinal displacement and rotation that describes transverse contraction. In all cases the crack is substituted by a dimensionless spring of the flexibility θ which is calculated by Castigliano's theorem and laws of the fracture mechanics (Dimarogonas). Using spectral element with crack allows analyzing high frequency excitation signal with small computational time and with high numerical accuracy. It is undoubtedly eligible feature and may have big influence on the modern damage monitoring techniques. A procedure of creating the dynamic stiffness matrix for the models is described in details. Numerical examples illustrating wave propagation process in rods for every model respectively are performed. The influence of damage on wave propagation is shown and a procedure to make use of those differences is presented. Comparison of crack identification results obtained for Love theory is included.

2. Rod theories

2.1. Elementary theory

A model of spectral element based on the elementary theory is presented in Fig.1.a. The element has the length L and the constant cross-section A . There are two nodes with one longitudinal degree of freedom per node.

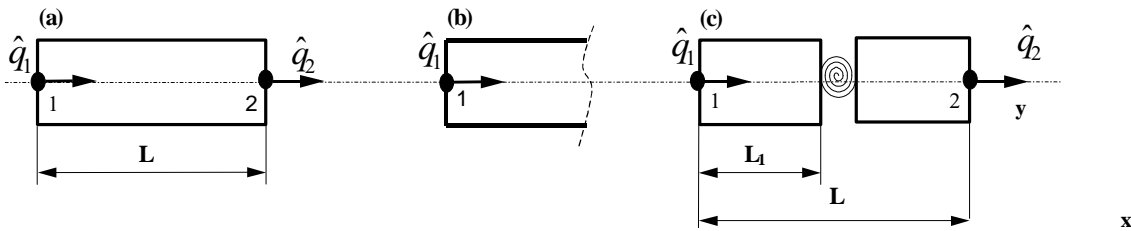


Figure 1. The spectral element models for the elementary and Love theories.

The elementary theory assumes that the axial deformations along the neutral axis of the rod are the same in all points of the cross-section, and also the transverse deflections are negligible. The differential equation of the problem can be written as follows:

$$EA \frac{\partial^2 u_0}{\partial x^2} - \rho A \frac{\partial^2 u_0}{\partial t^2} = 0 \quad (1)$$

with the boundary condition as:

$$u_0; \quad Q_u = EA \frac{\partial u_0}{\partial x} \quad (2)$$

where: u_0 is the average axial displacement, E denotes Young's modulus, A is the area of the cross-section of the rod and ρ is the density of the material.

For this theory the spectral element was established by Doyle [5]. The dynamic stiffness matrices for the two node spectral element K_{df} and the throw-off element K_{dt} can be presented in the following forms:

$$K_{df} = \frac{ikEA}{(1 - e^{-2ikL})} \begin{bmatrix} 1 + e^{-2ikL} & -2e^{-ikL} \\ -2e^{-ikL} & 1 + e^{-2ikL} \end{bmatrix} \quad (3)$$

$$K_{dt} = ikEA$$

where: k is the wave number calculated as a function of the frequency ω and material properties ρ , E :

$$k = \pm \omega \sqrt{\frac{\rho}{E}} \quad (4)$$

2.2. Love theory

The model of the spectral element based on the Love theory is also presented in Fig.1.a. The element has the same length and constant cross-section as the one calculated with elementary theory. Aforementioned element has two nodes with one longitudinal degree of freedom per node. The Love theory modification is based on the assumption that each material point of the rod has a transverse velocity. It means that the kinetic energy is affected by additional terms; nevertheless the strain energy is the same as of the elementary rod theory. The displacement field is also the same, and differential equation of the problem is only slightly modified, what can be expressed in the following form:

$$EA \frac{\partial^2 u_0}{\partial x^2} + v^2 \rho J \frac{\partial^2}{\partial x^2} \left(\frac{\partial^2 u_0}{\partial t^2} \right) - \rho A \frac{\partial^2 u_0}{\partial t^2} = 0 \quad (5)$$

with the boundary condition as:

$$u_0; \quad Q_u = EA \frac{\partial u_0}{\partial x} + v^2 \rho J \frac{\partial^2 u_0}{\partial t^2} \quad (6)$$

The term J denotes the polar moment of inertia of the rod's cross section, and v is the Poisson ratio of the material. The wave number for this model is given by relation:

$$k = \pm \omega \sqrt{\frac{\rho A}{EA - v^2 \rho J \omega^2}} \quad (7)$$

It should be noticed that the wave number k , in opposite to elementary theory, can be purely imaginary. In such case the transverse motion is absorbing all the input energy.

2.2.1. Rod spectral element for Love theory

The general longitudinal displacement of a rod can be written in the same form as for the elementary theory:

$$\hat{u}_0 = A_0 e^{-ikx} + B_0 e^{-ik(L-x)} \quad (8)$$

Constants A_0 and B_0 can be found from the following nodal conditions:

$$\begin{aligned} \hat{u}_0(x=0) &= \hat{q}_1 \\ \hat{u}_0(x=L) &= \hat{q}_2 \end{aligned} \quad (9)$$

which leads to the following system of equations:

$$\begin{bmatrix} A_0 \\ B_0 \end{bmatrix} = \begin{bmatrix} 1 & p \\ p & 1 \end{bmatrix}^{-1} \begin{bmatrix} \hat{q}_1 \\ \hat{q}_2 \end{bmatrix} \quad (10)$$

with $p = e^{-ikL}$.

The forces within the element can be expressed using formulas from Eq. (6) by differentiating the assumed displacements and calculating them for left end with $x=0$ and for the right end with $x=L-L_1$. Taking into account formulas for the axial displacement the nodal forces are given by the following expression:

$$\begin{bmatrix} \hat{F}_1 \\ \hat{F}_2 \end{bmatrix} = \begin{bmatrix} ik(-EA + \rho v^2 J \omega^2) & ik(-EA + \rho v^2 J \omega^2)p \\ ik(-EA + \rho v^2 J \omega^2)p & ik(-EA + \rho v^2 J \omega^2) \end{bmatrix} \begin{bmatrix} A_0 \\ B_0 \end{bmatrix} \quad (11)$$

Then using formulas for calculating constants A_0 and B_0 as a function of the nodal displacements, the relation between the nodal forces and the nodal displacements can be calculated. The square, symmetric matrix in this relation denotes the dynamic stiffness matrix K_{df} of the spectral element based on the Love theory.

2.2.2. Throw-off spectral element for Love theory

For the throw-off element based of the Love theory the general longitudinal displacement for a rod can be written is the same form as for the elementary theory:

$$\hat{u}_0 = A_0 e^{-ikx} \quad (12)$$

Constant A_0 can be found from the following nodal condition:

$$\hat{u}_0(x=0) = \hat{q}_1 \quad (13)$$

which leads to the equation:

$$A_0 = \hat{q}_1 \quad (14)$$

The forces within the element can be expressed using formulas from Eq. (6). The nodal forces can be found using the following nodal condition:

$$\hat{F}_1 = EA \frac{\partial \hat{u}_0}{\partial x} + v^2 \rho J \frac{\partial^2 \hat{u}_0}{\partial t^2} \quad \text{for } x=0 \quad (15)$$

Taking into account formulas for the axial displacements and the lateral contractions the nodal forces are given by the expression:

$$\hat{F}_1 = ik(-EA + \rho v^2 J \omega^2) \hat{q}_1 \quad (16)$$

The relation in the brackets in Eq. (16) denotes the dynamic stiffness matrix K_{dt} of the throw-off spectral element based on the Love theory.

2.2.1. Rod spectral element with transverse open and not propagating crack for Love theory

The spectral element for a cracked rod based on Love rod theory is presented in Fig.1.a. The element has two nodes and one degree of freedom per node. The longitudinal displacement u_0 can be expressed for the left and right part of the element as follows:

$$\hat{u}_{0,1}(x) = A_1 e^{-ikx} + B_1 e^{-ik(L_1-x)} \quad \text{for } x \in (0, L_1) \quad (17)$$

$$\hat{u}_{0,2}(x) = A_2 e^{-ik(L_1+x)} + B_2 e^{-ik[L-(L_1+x)]} \quad \text{for } x \in (0, L-L_1) \quad (18)$$

where k is the wave number given by Eq. (7).

The constants A_1 , B_1 , A_2 and B_2 can be found using traditional boundary conditions at the ends and special boundary conditions at the crack place where $x=L_1$ for $\hat{u}_{0,1}(x)$ and $x=0$ for $\hat{u}_{0,2}(x)$: the equality of longitudinal forces and the total change of displacements. Within the second mentioned boundary condition one includes the stiffness at the crack place (θ) for the first mode. The way of calculating the stiffness reduction due to crack appearance is shown in next paragraph. Taking into account formulas (17–18) and the boundary conditions the constants A_1 , B_1 , A_2 and B_2 can be expressed as a function of the nodal displacements in the following manner:

$$\begin{bmatrix} A_1 & B_1 & C_1 & D_1 \end{bmatrix}^T = W^{-1} \cdot \begin{bmatrix} \hat{q}_1 & 0 & 0 & \hat{q}_2 \end{bmatrix}^T \quad (19)$$

where:

$$W = \begin{bmatrix} 1 & e^{-ikL_1} & 0 & 0 \\ (-1 + ik\theta)e^{-ikL_1} & -1 - ik\theta & e^{-ikL_1} & e^{-ik(L-L_1)} \\ -ike^{-ikL_1} & ik & ike^{-ikL_1} & -ike^{-ik(L-L_1)} \\ 0 & 0 & e^{-ikL} & 1 \end{bmatrix} \quad (20)$$

The value of θ indicates the stiffness at the crack place calculated according the fracture mechanics law. The precise information is given by Krawczuk et al. The relationship between the nodal forces (Eq. (6)), calculated for the left end with ($x=0$) and for the right end with ($x=L-L_1$), and the nodal displacements denotes the dynamic stiffness matrix \mathbf{K}_{dyn} of the spectral element for the cracked rod, and is given by:

$$\begin{bmatrix} \hat{F}_1 \\ \hat{F}_2 \end{bmatrix} = K_{dyn} \cdot \begin{bmatrix} \hat{q}_1 \\ \hat{q}_2 \end{bmatrix} \quad (21)$$

with

$$K_{dyn} = (EA - v^2 \rho \cdot J \cdot \omega^2) \cdot \begin{bmatrix} ik & -ike^{-ikL_1} & 0 & 0 \\ 0 & 0 & -ike^{-ikL} & ik \end{bmatrix} \cdot W^{-1} \quad (22)$$

2.3. Mindlin–Herrmann theory (two-mode)

A model of a spectral element based on the Mindlin–Herrmann theory is presented in Fig.2.a. The element has the same geometry as in two previously described cases. It has also two nodes with two degrees of freedom per node (the longitudinal displacement and the rotation). The Mindlin–Herrmann theory can be developed taking into account independent shearing deformation due to transverse displacement.

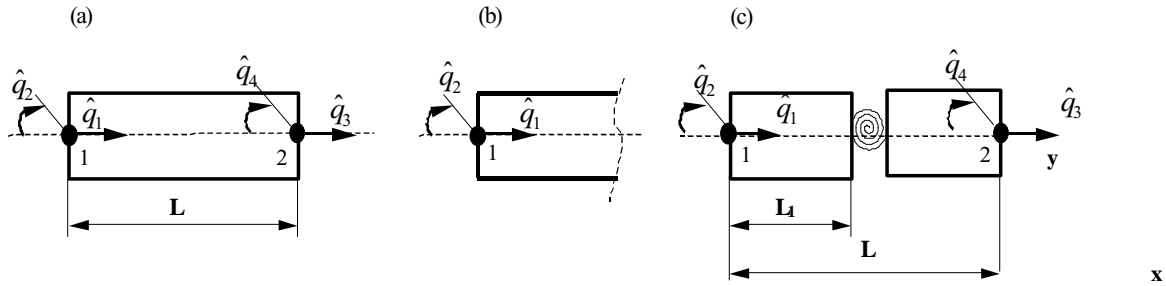


Figure 2. The spectral element models for the Mindlin–Herrmann theory.

The displacements in Mindlin–Herrmann theory of rods are assumed as follows (Doyle [5]):

$$\begin{aligned} u(x, y) &= u_0(x) \\ v(x, y) &= \psi_0(x) \cdot y \end{aligned} \quad (23)$$

where: y_0 denotes the transverse contraction.

This approach takes into account the lateral displacements, but ignores the nonuniform distribution of the axial displacement in the cross section of the rod. The differential equations for the Mindlin–Herrmann theory, governing the rod vibration problem, are as follows (Doyle [5]):

$$\begin{aligned} (2\mu + \lambda)A \frac{\partial^2 u_0}{\partial x^2} + \lambda A \frac{\partial \psi_0}{\partial x} &= \rho A \frac{\partial^2 u_0}{\partial t^2} - q \\ \mu I K_1 \frac{\partial^2 \psi_0}{\partial x^2} - (2\mu + \lambda)A \psi_0 - \lambda A \frac{\partial u_0}{\partial x} &= \rho I K_2 \frac{\partial^2 \psi_0}{\partial t^2} \end{aligned} \quad (24)$$

with the associated boundary conditions (at each end of the rod)

$$\begin{aligned} u_0: \quad Q_u &= (2\mu + \lambda)A \frac{\partial u_0}{\partial x} + \lambda A \psi_0 \\ \psi_0: \quad Q_\psi &= \mu I K_1 \left(\frac{\partial \psi_0}{\partial x} \right) \end{aligned} \quad (25)$$

where: $\mu = \frac{E}{2(I + \nu)}$, $\lambda = \frac{\nu E}{(I + \nu)(I - 2\nu)}$ and I is the geometrical moment of the rod's cross section.

Parameters K_1 and K_2 are calculated from the formulas:

$$K_1 = \frac{I2}{\pi^2}, \quad K_2 = K_1 \left(\frac{I + \nu}{0.87 + I.12\nu} \right)^2 \quad (26)$$

They are a set of coupled equations for the longitudinal displacement and lateral contraction. Since there are two dependent variables u_0 and y_0 , and the coefficients are constant, to obtain the spectrum relation one assumes solutions in the form:

$$u_0 = U e^{-i(kx - \omega t)}, \quad \psi_0 = \Psi e^{-i(kx - \omega t)} \quad (27)$$

After the substitution into differential equations give the system to be satisfied as:

$$\begin{bmatrix} -(2\mu + \lambda)Ak^2 + \rho A\omega^2 & -ik\lambda A \\ ik\lambda A & -\mu IK_1 k^2 - (2\mu + \lambda)A + \rho IK_2 \omega^2 \end{bmatrix} \begin{bmatrix} U \\ \Psi \end{bmatrix} = \begin{bmatrix} 0 \\ 0 \end{bmatrix} \quad (28)$$

Setting the determinant to zero gives the characteristic equation for determining k as:

$$a_2 k^4 + a_1 k^2 + a_0 = 0 \quad (29)$$

where:

$$\begin{aligned} a_2 &= \mu AIK_1 (2\mu + \lambda) \\ a_1 &= [4\mu(\mu + \lambda)A^2 - \rho IK_2 \omega^2 (2\mu + \lambda)A - \rho A\omega^2 \mu IK_1] \\ a_0 &= -\rho A\omega^2 [A(2\mu + \lambda) - \rho IK_2 \omega^2] \end{aligned} \quad (30)$$

This characteristic equation is quadratic in k^2 and therefore, there are two-mode pairs in contrast to the single pair of the elementary and Love theories.

2.3.1. Rod spectral element for the Mindlin–Herrmann theory

The general longitudinal displacement and rotation of a rod can be written as:

$$\begin{aligned} \hat{u}_0 &= A_0 R_1 e^{-ik_1 x} + B_0 R_2 e^{-ik_2 x} - C_0 R_1 e^{-ik_1(L-x)} - D_0 R_2 e^{-ik_2(L-x)} \\ \hat{\Psi}_0 &= A_0 e^{-ik_1 x} + B_0 e^{-ik_2 x} + C_0 e^{-ik_1(L-x)} + D_0 e^{-ik_2(L-x)} \end{aligned} \quad (31)$$

where R_i are the amplitude ratios given by:

$$R_i = \frac{ik_i \lambda A}{-(2\mu + \lambda)Ak_i^2 + \rho A\omega^2}, \quad i = 1, 2 \quad (32)$$

Constants A_0 , B_0 , C_0 and D_0 can be found from the following nodal conditions:

$$\begin{aligned} \hat{u}_0(x=0) &= \hat{q}_1, \quad \hat{\Psi}_0(x=0) = \hat{q}_2 \\ \hat{u}_0(x=L) &= \hat{q}_3, \quad \hat{\Psi}_0(x=L) = \hat{q}_4 \end{aligned} \quad (33)$$

The forces within the element can be expressed by differentiating formulas from Eq. (26) and by using the following nodal conditions one obtains:

$$\begin{aligned} \hat{F}_1 &= (2\mu + \lambda)A \frac{\partial \hat{u}_0}{\partial x} + \lambda A \Psi_0 \quad \text{for } x=0, \quad \hat{F}_2 = \mu IK_1 \left(\frac{\partial \hat{\Psi}_0}{\partial x} \right) \quad \text{for } x=0, \\ \hat{F}_3 &= (2\mu + \lambda)A \frac{\partial \hat{u}_0}{\partial x} + \lambda A \Psi_0 \quad \text{for } x=L, \quad \hat{F}_4 = \mu IK_1 \left(\frac{\partial \hat{\Psi}_0}{\partial x} \right) \quad \text{for } x=L \end{aligned} \quad (34)$$

Taking into account formulas for the axial displacement and rotation with the formulas for calculating constants A_0 , B_0 , C_0 and D_0 it is possible to express the nodal forces as a function of nodal displacements. The relation between the nodal displacements and the nodal forces contains the square, symmetric matrix, which is the dynamic stiffness matrix K_{df} of the spectral element based on the Mindlin–Herrmann theory.

2.3.2. Throw-off spectral element for the Mindlin–Herrmann theory

For the throw-off element (Fig.2.b) based on the Mindlin–Herrmann theory the axial displacement and rotation are given by:

$$\begin{aligned} \hat{u}_0 &= A_0 R_1 e^{-ik_1 x} + B_0 R_2 e^{-ik_2 x} \\ \hat{\Psi}_0 &= A_0 e^{-ik_1 x} + B_0 e^{-ik_2 x} \end{aligned} \quad (35)$$

Constants A_0 and B_0 can be found from the following nodal conditions:

$$\hat{u}_0(x=0) = \hat{q}_1, \quad \hat{\Psi}_0(x=0) = \hat{q}_2 \quad (36)$$

The forces within the element can be expressed using formulas from Eq. (25). The nodal forces can be found using the following nodal conditions:

$$\hat{F}_1 = (2\mu + \lambda)A \frac{\partial \hat{u}_0}{\partial x} + \lambda A \Psi_0 \quad \text{for } x=0, \quad \hat{F}_2 = \mu I K_I \left(\frac{\partial \hat{\Psi}_0}{\partial x} \right) \quad \text{for } x=0, \quad (37)$$

With the formulas for calculating the axial displacement and rotation and using formulas for calculating constants A_0 and B_0 as a function of the nodal displacements the relation between the nodal forces and the nodal displacements can be calculated. The square, symmetric matrix in this formula is the dynamic stiffness matrix K_{dt} of the throw-off spectral element based on the Mindlin–Herrmann theory.

2.3.3. Rod spectral element with transverse open and not propagating crack for the Mindlin–Herrmann theory

The spectral element for a cracked rod based on Mindlin–Herrmann rod theory is presented in Fig.2.c. The element has two nodes and two degrees of freedom per node. The longitudinal displacement u_0 and rotation y_0 can be expressed for the left and right part of the element as follows:

$$\begin{aligned} \hat{u}_{0,1} &= A_1 R_1 e^{-ik_1 x} + B_1 R_2 e^{-ik_2 x} - C_1 R_1 e^{-ik_1(L_1-x)} - D_1 R_2 e^{-ik_2(L_1-x)} & \text{for } x \in (0, L_1) \\ \hat{\Psi}_{0,1} &= A_1 e^{-ik_1 x} + B_1 e^{-ik_2 x} + C_1 e^{-ik_1(L_1-x)} + D_1 e^{-ik_2(L_1-x)} & \text{for } x \in (0, L_1) \\ \hat{u}_{0,2} &= A_2 R_1 e^{-ik_1(L_1+x)} + B_2 R_2 e^{-ik_2(L_1+x)} - C_2 R_1 e^{-ik_1(L-(L_1+x))} - D_2 R_2 e^{-ik_2(L-(L_1+x))} & \text{for } x \in (L_1, L-L_1) \\ \hat{\Psi}_{0,2} &= A_2 e^{-ik_1(L_1+x)} + B_2 e^{-ik_2(L_1+x)} + C_2 e^{-ik_1(L-(L_1+x))} + D_2 e^{-ik_2(L-(L_1+x))} & \text{for } x \in (L_1, L-L_1) \end{aligned} \quad (38)$$

with R_i defined by Eq.(32) and k_1 and k_2 denoting the wave numbers which are a solution of Eq. (29). In order to calculate unknown constants $A_1, B_1, C_1, D_1, A_2, B_2, C_2$ and D_2 the following boundary conditions are used:

- for the left end of the element ($x=0$):

$$\hat{u}_{0,1}(x) = \hat{q}_1, \quad \hat{\Psi}_{0,1}(x) = \hat{q}_2 \quad (40)$$

- at the crack location ($x=L_1$ for $\hat{u}_{0,1}(x), \hat{\Psi}_{0,1}(x)$ and $x=0$ for $\hat{u}_{0,2}(x), \hat{\Psi}_{0,2}(x)$):

$$\hat{u}_{0,2}(x) - \hat{u}_{0,1}(x) = \theta^* \frac{\partial \hat{u}_{0,1}(x)}{\partial x} + \lambda \hat{\Psi}_{0,1}(x) \quad (42)$$

$$(2\mu + \lambda)A \frac{\partial \hat{u}_{0,1}(x)}{\partial x} + \lambda A \hat{\Psi}_{0,1}(x) = (2\mu + \lambda)A \frac{\partial \hat{u}_{0,2}(x)}{\partial x} + \lambda A \hat{\Psi}_{0,2}(x) \quad (43)$$

$$\hat{\Psi}_{0,1}(x) = \hat{\Psi}_{0,2}(x) \quad (44)$$

$$\frac{\partial \hat{\Psi}_{0,1}(x)}{\partial x} = \frac{\partial \hat{\Psi}_{0,2}(x)}{\partial x} \quad (45)$$

- for the right end of the element ($x=L-L_1$):

$$\hat{u}_{0,2}(x) = \hat{q}_3, \quad \hat{\Psi}_{0,2}(x) = \hat{q}_4 \quad (46)$$

where \hat{q}_1, \hat{q}_3 denote the nodal axial displacements, \hat{q}_2, \hat{q}_4 are nodal rotations and $\theta^* = c(2\mu + \lambda)A$.

Taking into account formulas (39) and the boundary conditions given by Eqs. (41–46) the constants $A_1, B_1, C_1, D_1, A_2, B_2, C_2$ and D_2 can be expressed as a function of nodal displacements.

Nodal forces are given by the following formulas:

- for the left end of the element ($x=0$):

$$\hat{F}_1 = (2\mu + \lambda)A \frac{\partial \hat{u}_{0,1}(x)}{\partial x} + \lambda A \hat{\Psi}_{0,1}(x) \quad (47)$$

$$\hat{F}_2 = \mu I K_I \left(\frac{\partial \hat{\Psi}_{0,1}(x)}{\partial x} \right)$$

- for the right end of the element ($x=L-L_1$):

$$\hat{F}_3 = (2\mu + \lambda)A \frac{\partial \hat{u}_{0,2}(x)}{\partial x} + \lambda A \hat{\Psi}_{0,2}(x) \quad (48)$$

$$\hat{F}_4 = \mu I K_I \left(\frac{\partial \hat{\Psi}_{0,2}(x)}{\partial x} \right)$$

Then using the formulas for calculating constants $A_1, B_1, C_1, D_1, A_2, B_2, C_2$ and D_2 as a function of the nodal displacements, the relation between the nodal forces and the nodal displacements can be calculated. The square, symmetric matrix in this relation denotes the dynamic stiffness matrix K_{dyn} of the cracked spectral element based on the Mindlin–Herrmann rod theory.

3. Exemplary results

This section is devoted to comparison of results obtained for different rod theories. All numerical tests were done for a cantilever steel rod with such geometrical dimensions: length 4 m, width 0,02 m, height 0,02 m. The following material properties are utilised: Young’s modulus 210 GPa, Poisson ratio 0,3 and density 7850 kg/m^3 . Two different signals are used as the source of propagating wave. Fig.4 illustrates the comparison of analysed signal shapes, duration times and their FFT. Every of the signal presented is co called ‘package’ obtained from the multiplication of a triangle and a sinusoidal function. Signal marked as (a) is the slower tested and lasts for 0,3 ms. It allows to excite waves of frequency up to 80 kHz. The faster of used and presented signals (case (b)) lasts for 0,15 ms and lets to operate on the biggest frequency range – up to 160 kHz.

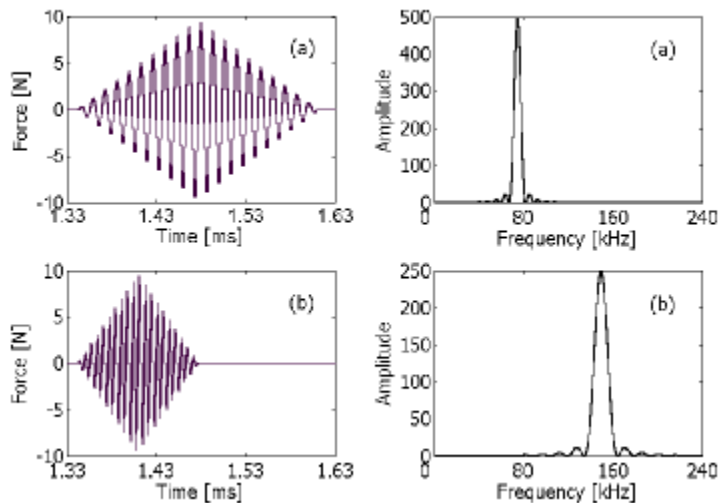


Fig. 4. Comparison of tested excitation signals in time and frequency domains.

The next two figures present comparison of reflected signals obtained for the elementary and modified theories. For better illustration of differences the accelerations calculated for all the models are normalized according to their maximum value. Figure 5 presents comparison of results obtained for the excitation signals tested. The first plot (Fig.5.(a)) illustrates differences in reflected signal obtained for elementary and Love theories for the slower signal from Fig.4(a), the second plot (Fig.5.(b)) shows differences for the faster signal shown at Fig.4(b). As it can be seen more visible differences between results can be observed for higher frequencies excited by the input signal.

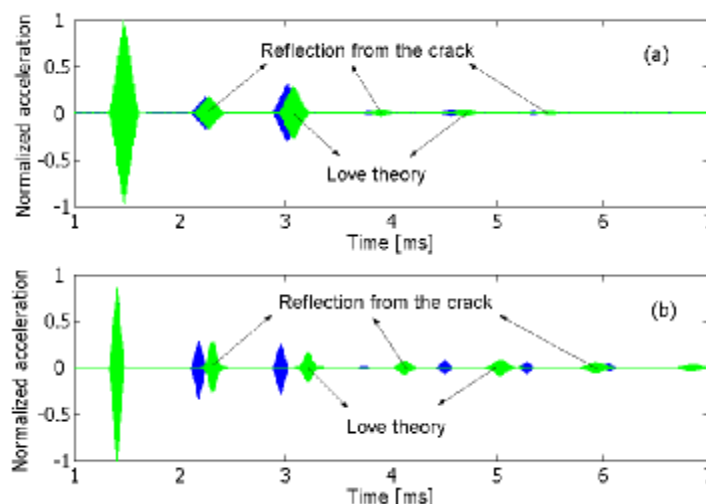


Figure 5. Reflected signals obtained for the elementary and Love theories for the slower excitation signal (a) for the faster excitation signal (b).

Figure 6 presents the comparison of results obtained for both examined excitation signals with the models based on elementary and Mindlin–Herrmann rod theories. The meaning of the plots is the same as in Fig.5. The differences between results for the models are much more visible when the input signal excites higher frequencies. As it can be noticed on Fig.6(b) for the Mindlin–Herrmann theory additional reflections appeared, which were not present in case of the elementary or Love theories.

A practical remark is that before choosing a model the analysis of wave numbers for specific material and geometrical data is required. When the excitation signal frequency does not excite higher modes the Love theory gives very good results. In other case, that is for signal frequencies, which excite higher modes, the Mindlin–Herrmann theory should be applied.

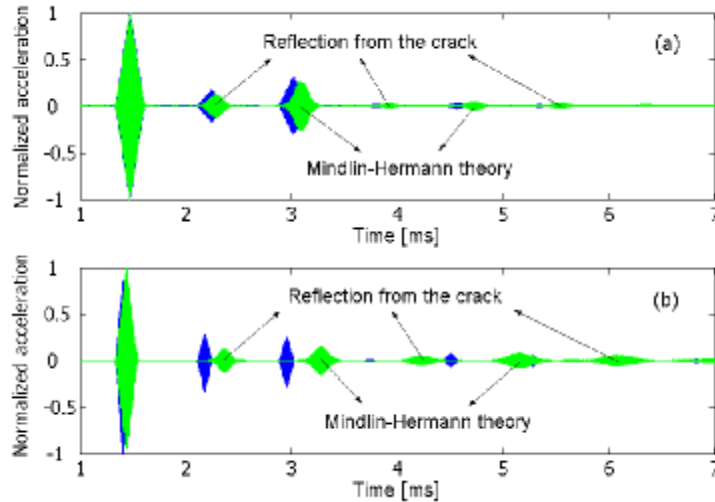


Figure 6. Reflected signals obtained for the elementary and Mindlin–Herrmann theories for the slower excitation signal (a) for the faster excitation signal (b).

4. Discontinuity identification

From the analysis done it follows that the reflections from different discontinuities appear shifted in time, especially in case of changing material properties. It was also noticed that there are phase shifts between the excitation signals and reflections from discontinuity. On that bases an attempt to identify the existence of discontinuity is performed. For that purpose the cross correlation function was utilized, which gives information about the phase shift in the signal. The mathematical formula showing the relation between the reference or excitation signal (x_{ref}) and the reflection from discontinuity, for a certain time delay (τ) is given by:

$$R(\tau) = \sum_{t=1}^N x_{ref}(t)x(t+\tau), \quad (60)$$

where N is the samples number. When the cross correlation function is positive – indicates the same phases of examined signals, then it is negative – there is a phase shift between signals analysed. The second analysed value was the signal power which is given by the following relation:

$$x_{pwr} = \sum_{n=1}^N x^2(n) = \sum_{n=1}^N |x(n)|^2 \quad (61)$$

where N is the samples number.

Changes of the cross correlation function (CCF), calculated for two first reflections of the examined signals are presented on Fig. 7. While the numerical simulation the relative crack depth was changed from 0,5% to 50% of the rod height. Fig. 7 presents the CCF obtained all described rod theories for the slower signal (Fig. 4(a)), whereas the Fig. 8 illustrates the similar changes but calculated with the faster signal (Fig. 4(b)). On every plot proper marks are performed to indicate the theory from which comes the curve. After analysing the CCF calculated for both signals one can conclude that in case of utilizing the faster signal the changes of the factor seem to be sharper compared with those calculated for the slower one. Important influence can be noticed regarding the theory – analysis of signal with higher frequency range is better when Mindlin – Herrmann theory is applied.

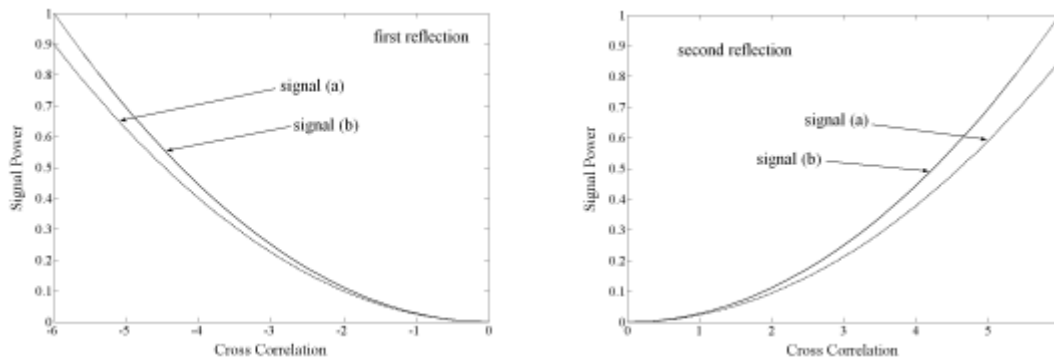


Figure 6. Changes of the Cross Correlation function for the excitation signal (a) and for the excitation signal (b).

5. Conclusions

The paper presents wave propagation in rods with fatigue cracks. Analyzed responses are obtained for three rod theories: the elementary, the Love and the Mindlin – Herrmann rod theory. All solutions are obtained with spectral element method. As concluding set of remarks it should be pointed out that the excitation frequency influences the sensitivity of the system. The bigger the frequency is the smaller damage can be found. However it is important to keep in mind that higher frequencies are properly modeled with theories that consider the presence of higher modes excited with very fast signals. Reassuring the bigger excitation signal frequency is the better damage identification sensitivity, however one needs to remember about the equipment limitations while practical implementations.

Second important conclusion from the paper is that due to the crack occurrence certain differences appear in a response signal. They come from additional reflections from the damaged area, which is of course sort of discontinuity. The differences are utilized for calculation cross correlation factor, which may be helpful for damage identification. Knowing that damage influences the damage identification function it would be possible to indicate damage presence on the bases of the measured signal only. Adequate simple example is shown. Although the proposed procedure is applied on a simple rod element only the idea is to widen the method on more complicated elements. This task, as well the experimental verification of proposed models, is the main subject of the authors' present research activities.

6. Acknowledgments

M. Palacz would like to thank the Foundation for Polish Science for being granted the Scholarship for Young Scientists edition 2003.

7. References

- Bathe K.J., 1982, „Finite Element Procedures in Engineering Analysis”. Prentice Hall, Englewood Cliffs.
- Chang F-K., 1997,1999, 2001, „Structural Health Monitoring: Current Status and Perspectives”. Edited by F.-K. Chang, Technomic Publishing Co., Inc., Lancaster – Basel.
- Cheung Y.K., 1976, „Finite Strip Method in Structural Analysis”. Pergamon Press, New York.
- Dimarogonas A.D., Paipetis S.A., 1983, „Analytical methods in rotor dynamics”, Applied Science Publishers, London.
- Doyle J. F., 1997, „Wave Propagation in Structure”s, New York, Springer-Verlag.
- Krawczuk M., Palacz M., Ostachowicz W., 2003, „The dynamic analysis of cracked Timoshenko beam by the spectral element method.” *Journal of Sound and Vibration*, 264, 1139-1153.
- Mahapatra D.R., Golpalakrishnan S., 2003, „A spectral finite element model for analysis of axial – flexural – shear coupled wave propagation in laminated composite beams.” *Computers and Structures*, 59, 67 – 88.
- Palacz M., Krawczuk M., 2002, „Analysis of Longitudinal Wave Propagation in a Cracked Rod by the Spectral Element Method.” *Computers and Structures*, 80, 1809 – 1816.
- Redwood M., 1960, „Mechanical Waveguides.” Pergamon Press, New York.
- Tada H., Paris P.C., Irwin G.R. 1973, „The Stress Analysis of Cracks Handbook.” Del Research Corporation.

9. Responsibility notice

The authors are the only responsible for the printed material included in this paper.